Received: 3 April 2022 | Accepted: 21 October 2022

DOI: 10.1111/1365-2656.13847

Journal of Animal Ecology | BRITISH ECOLOGICAL SOCIETY

RESEARCH ARTICLE

Active Remote Sensing for Ecology and Ecosystem Conservation

LiDAR reveals a preference for intermediate visibility by a forest-dwelling ungulate species

Xin Zong[1] | Tiejun Wang[1] | Andrew K. Skidmore[1,2] | Marco Heurich[3,4,5]

[1]Faculty of Geo-Information Science and Earth Observation (ITC), University of Twente, Enschede, The Netherlands

[2]Department of Environmental Science, Macquarie University, Sydney, Australia

[3]Department of Conservation and Research, Bavarian Forest National Park, Grafenau, Germany

[4]Chair of Wildlife Ecology and Management, University of Freiburg, Freiburg, Germany

[5]Institute for Forestry and Wildlife Management, Inland Norway University of Applied Science, Koppang, Norway

Correspondence
Xin Zong
Email: x.zong@utwente.nl

Funding information
China Scholarship Council, Grant/Award Number: 201704910852; H2020 European Research Council, Grant/Award Number: 834709 and H2020-EU.1.1.; 'Data Pool Initiative' of the Bohemian Forest Ecosystem

Handling Editor: Carlos Alberto Silva

Abstract

1. Visibility (viewshed) plays a significant and diverse role in animals' behaviour and fitness. Understanding how visibility influences animal behaviour requires the measurement of habitat visibility at spatial scales commensurate to individual animal choices. However, measuring habitat visibility at a fine spatial scale over a landscape is a challenge, particularly in highly heterogeneous landscapes (e.g. forests). As a result, our ability to model the influence of fine-scale visibility on animal behaviour has been impeded or limited.
2. In this study, we demonstrate the application of the concept of three-dimensional (3D) cumulative viewshed in the study of animal spatial behaviour at a landscape level. Specifically, we employed a newly described approach that combines terrestrial and airborne light detection and ranging (LiDAR) to measure fine-scale habitat visibility (3D cumulative viewshed) on a continuous scale in forested landscapes. We applied the LiDAR-derived visibility to investigate how visibility in forests affects the summer habitat selection and the movement of 20 GPS-collared female red deer *Cervus elaphus* in a temperate forest in Germany. We used integrated step selection analysis to determine whether red deer show any preference for fine-scale habitat visibility and whether visibility is related to the rate of movement of red deer.
3. We found that red deer selected intermediate habitat visibility. Their preferred level of visibility during the day was substantially lower than that of night and twilight, whereas the preference was not significantly different between night and twilight. In addition, red deer moved faster in high-visibility areas, possibly mainly to avoid predation and anthropogenic risk. Furthermore, red deer moved most rapidly between locations in the twilight.
4. For the first time, the preference for intermediate habitat visibility and the adaption of movement rate to fine-scale visibility by a forest-dwelling ungulate species at a landscape scale was revealed. The LiDAR technique used in this study offers fine-scale habitat visibility at the landscape level in forest ecosystems, which would be of broader interest in the fields of animal ecology and behaviour.

KEYWORDS
fine-scale visibility, habitat selection, integrated step selection analysis, movement rate, red deer, viewshed

1 | INTRODUCTION

Visual information plays a significant and diverse role in animals' behaviour and fitness. For prey species, visual information from the environment can affect their ability to remain hidden or to detect approaching predators, thereby avoiding predation (Camp et al., 2012; Embar et al., 2011; Lima & Dill, 1990). On the other hand, predators relying on the vision for hunting can locate their prey and use appropriate predation strategies that increase their chance of success (Andersson et al., 2009; Hopcraft et al., 2005; Loarie et al., 2013). Visibility is the environmental property that provides lines of sight enabling an individual to visually detect prey or predators and has often been used to quantify what an animal can potentially see (Aben et al., 2018; Camp et al., 2013). Visibility has been shown to alter predation risk imposed by predators or perceived by prey species and thus affect an animal's habitat selection for foraging (Dupke et al., 2017; Embar et al., 2011), hunting (Loarie et al., 2013), reproduction (Rearden et al., 2011), resting (Adrados et al., 2008; Davies, Marneweck, et al., 2016) and mating (Alonso et al., 2012), as well as its movement (Frair et al., 2005; Proffitt et al., 2009). Therefore, further improvements in understanding animal spatial behaviour would greatly benefit from considering environmental visibility.

Behavioural responses of animals via habitat selection or movement occur at multiple scales (Johnson, 1980; Wiens, 1989). Therefore, understanding how visibility influences animal behaviour requires measuring habitat visibility at spatial scales that are commensurate with the choices made by individual animals. However, there has always been a mismatch between the scales (e.g. plant, patch and landscape) at which animals make decisions and the resolution of the data on habitat visibility available across these same spatial scales. This mismatch becomes more severe at the fine end of this scale spectrum (Olsoy et al., 2014). Recent advances in sensor tracking technology (e.g. GPS) allow the recording of movement paths of individual animals at a much finer spatiotemporal scale than previously possible, thus providing a new and valuable opportunity to investigate the direct interaction of a single animal with its surroundings. However, it is a challenge to measure habitat visibility at a fine spatial scale linked to the high-resolution locational data of animals across a landscape, particularly in highly heterogeneous landscapes (e.g. forests) (Zong et al., 2021a). As a result, our ability to model the influence of fine-scale visibility on animal behaviour has been impeded or limited.

Traditional field methods of measuring fine-scale visibility in terrestrial ecosystems such as forests and grasslands are to observe or photograph obscurity boards or poles and determine the percentage covered by environmental features, often vegetation (Higgins et al., 1996). However, a key limitation of these approaches is that visibility will be obtained only from a predetermined viewpoint and in limited directions. Moreover, the sampling efficiency of these conventional approaches is low and measurements are hard to replicate. The 360° range of visibility from an observation point is commonly referred to as a viewshed (Tandy, 1967). In the fields of landscape planning and archaeology, the aggregate visibility from multiple observation points has been conceptualized by the term cumulative viewsheds. This concept has been implemented in most geographic information system (GIS) software to calculate viewsheds across digital elevation surfaces. However, digital elevation surfaces are not suitable for assessing fine-scale visibility in forests, as they do not contain understorey information. As such, viewshed analysis functions in GIS have not been widely adopted in animal ecology research (Aben et al., 2018).

Light detection and ranging (LiDAR) technology provides a good opportunity to develop a more effective and efficient approach to estimating visibility in forests due to its capability of providing horizontal and vertical information for different canopy layers (Ciuti et al., 2018). Terrestrial laser scanning (TLS, also known as terrestrial LiDAR) can generate highly dense laser returns, especially in the lower vegetation layers (e.g. canopy base, understorey and terrain). Hence, it can capture the three-dimensional (3D) structure at a fine spatial resolution (<2 cm), allowing the 3D structure of forest stands to be represented with substantial details. Recent studies have proven the success of the TLS technique in rapidly estimating fine-scale visibility in forests (Lecigne et al., 2020; Olsoy et al., 2014; Zong et al., 2021b). 3D viewsheds and cumulative viewsheds can be generated using TLS-based methods (Lecigne et al., 2020; Zong et al., 2021a). Extended from a gridded digital surface in GIS to a 3D space, a 3D viewshed is represented by all voxels of a voxelized space that are connected by the lines of sight to the viewpoint. A 3D cumulative viewshed is created by repeatedly calculating the 3D viewsheds from multiple viewpoints, then summing them into a single 3D viewshed. This determines how well a voxel can be seen from many viewpoints. Furthermore, TLS-based methods can improve sampling efficiency compared to traditional field methods that rely on obscurity boards. However, the estimates of fine-scale visibility derived from obscurity board-based and TLS-based methods are both ground based at a plot level, and therefore are site specific with limited spatial coverage. It is impractical to replicate these measurements from many locations across a landscape to obtain a continuous visibility map at a landscape scale.

Due to the absence of methods to continuously characterize the habitat visibility of animals, surrogate metrics that can index visibility to some extent have often been used in studies analysing the influence of visibility on animal behaviour. These metrics include land cover type, topography, vegetation cover and vegetation density (Acebes et al., 2013; Filla et al., 2017; Johnson et al., 2000; Salvatori et al., 2022). However, these are not physical measurements of real

visibility, even though they are related to visibility. Moreover, proxies for visibility cannot account for the effects of the height of animal eyes. Airborne laser scanning (ALS, also known as airborne LiDAR) can provide information about 3D vegetation structure and the underlying terrain surface at a landscape scale and has been used to map visibility for analyses of animal habitat selection in recent studies (Aben et al., 2018; Davies et al., 2021; Davies, Marneweck, et al., 2016; Davies, Tambling, et al., 2016; Loarie et al., 2013). However, in these studies, airborne LiDAR was used to model the upper (forest) canopy surfaces from which viewsheds were calculated at limited sites of interest, ignoring visual obstruction of the understorey vegetation. Rather than directly calculating viewsheds from ALS data, Zong et al. (2021a) extracted predictive metrics from ALS data over a temperate forest and upscaled the 3D cumulative viewshed derived from TLS at the ground level to the landscape level. Thus, the integration of TLS and ALS has proven to be a viable method to produce a high-resolution wall-to-wall map of habitat visibility in forested landscapes.

Compared to traditional measurements (e.g. scores derived from obscurity boards), 3D cumulative viewsheds can provide representations of an animal's potential visual space with much higher resolution. Moreover, traditional visibility measurements are viewpoint specific and thus change when the viewpoint is moved. By contrast, a 3D cumulative viewshed is derived from the integration of 3D viewsheds from multiple viewpoints. It can therefore account for the movement of viewpoints and comprehensively quantify the relative visibility of an area of interest in a landscape. Although some previous studies have highlighted the potential of the viewshed approach for animal ecology (Lecigne et al., 2020, Olsoy et al., 2014, Zong et al., 2021a) and have called for the study of the 'viewshed ecology' (Aben et al., 2018), 3D cumulative viewshed is a new concept that has not yet been applied in animal ecology research. The 3D cumulative viewshed, integrated with animal position data, provides an opportunity to characterize the influence of visual information on animal behaviour and fitness. It can promote the use of the concept of viewshed (visibility) in animal ecology research.

As a forest-dwelling herbivore, and also one of the most widely distributed deer in the world, the red deer *Cervus elaphus* is known to be susceptible to predation and thus sensitive to habitat visibility. First, visibility can affect habitat use patterns in red deer. For example, red deer more often feed in open habitats (e.g. meadows) because reduced canopy shading means that forage is more abundant and of better quality in open habitats than in covered habitats (mainly forests; Godvik et al., 2009). On the other hand, red deer more often rest in forests to avoid predation risk from rifle hunters who rely on long lines of sight in open habitats (Lone et al., 2015). Second, there is evidence that red deer adapt their movement behaviour to habitat visibility. A notable example is that when hunted, red deer were observed to flee longer distances and move faster in more open areas where their visibility to predators/hunters is greater (Jarnemo & Wikenros, 2014). One of the impediments to examining the relationships between environmental visibility and the use of space by red deer in previous studies was the binary categorization of visibility as 'open' or 'closed'. For example, the levels of habitat visibility were frequently represented by land cover type. The visibility levels of various forested habitats were usually assumed to be lower and thus categorized as closed, whereas the visibility levels of meadow habitats were assumed to be higher and thus categorized as open (Godvik et al., 2009). However, visibility is not just open (high) or closed (low), it occurs at a range of values in a landscape. Currently, how red deer continuously select areas of varying visibility and adapt their movement behaviour accordingly in a landscape remains largely unexplored.

Here, we demonstrate the application of the concept of 3D cumulative viewshed in the study of animal spatial behaviour at the landscape level. Specifically, we employed the newly described LiDAR-based fine-scale visibility approach to investigate how visibility in forests influences the summer habitat selection and the movement of 20 GPS-collared female red deer in a temperate forest in Germany. In this study, we have two specific aims and associated hypotheses: (1) To determine the preference of red deer for fine-scale visibility and test whether the preference differs depending on the time of day considering the daily activity pattern of red deer. We hypothesized that red deer would prefer intermediate habitat visibility and their preferred visibility during the day would be lower than that of night and twilight; (2) To examine the relationship between visibility and the movement rate of red deer. We hypothesized that red deer will move faster in high-visibility areas throughout the day and night.

2 | MATERIALS AND METHODS

2.1 | Study site

The study site, Bavarian Forest National Park (BFNP, 49°3′19″N, 13°12′9″E), is located in Southeast Germany (Figure 1). This mountainous park extends over an area of approximately 240 km^2, with elevations ranging from 590 to 1553 m above sea level. The mean annual precipitation of BFNP varies from 965 to 1860 mm and the mean annual air temperature ranges from 3.9 to 8.6°C (Röder et al., 2010). Snow cover can last up to 7 months per year on the mountain tops (October to May) and 5 months per year in the valleys (November–April). Ninety-eight percent of the area in BFNP is covered by a mixed temperate forest, and the main vegetation types found in the park include deciduous forest, coniferous forest, mixed forest, meadows and lying or standing deadwood. The dominant tree species are Norway spruce *Picea abies* (67%) and European beech *Fagus sylvatica* (24.5%), with other tree species (e.g. *Abies alba*, *Acer pseudoplatanus*, *Fraxinus excelsior* and *Sorbus aucuparia*) making up the remaining 10% of forest (Cailleret et al., 2014). In the last decades, the infestation of Norway spruce with spruce bark beetles *Ips typographus* and wind throws have resulted in large swathes of standing or lying deadwood (Fahse & Heurich, 2011).

Red deer use the whole area of the national park in summer. The majority of red deer spend the winter in four enclosures established

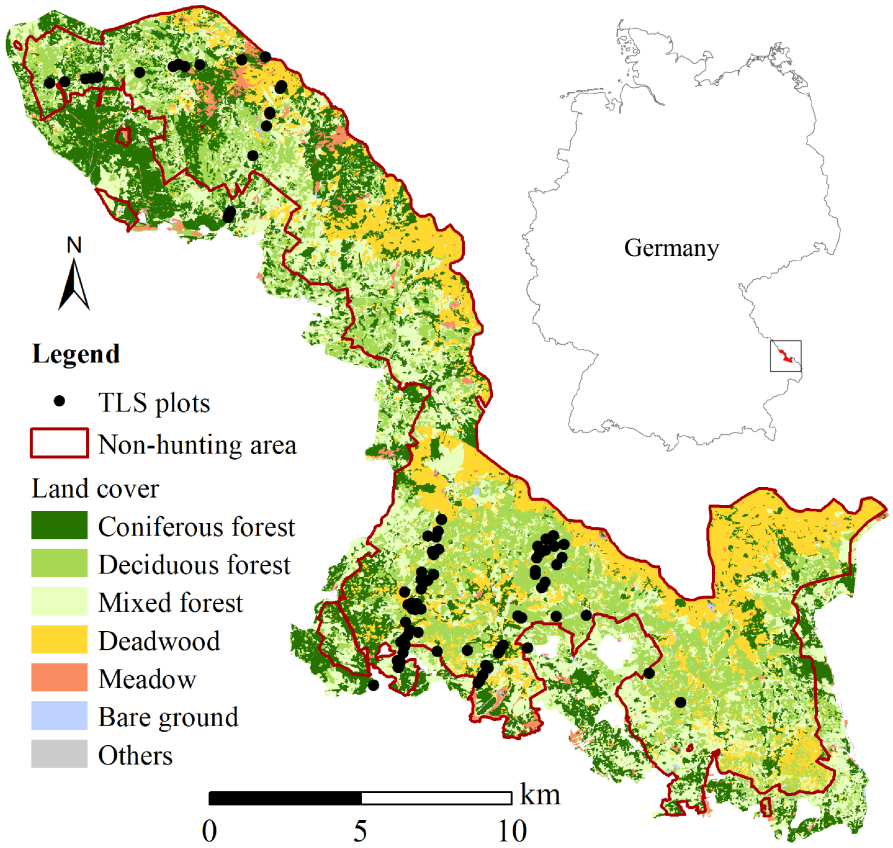

FIGURE 1 The location of the study site, the Bavarian Forest National Park, Germany.

within the park where they are fed and where their numbers are controlled (Möst et al., 2015). Hunting of red deer is prohibited within the non-hunting area of the national park, while outside the non-hunting area, red deer are occasionally hunted to protect the forest enterprises and agricultural areas at lower altitudes from damage (Möst et al., 2015). The Eurasian lynx *Lynx lynx* is the only large carnivore species inhabiting the study area permanently, and red deer, mainly young and female individuals, make up about 17% of lynx kills (Belotti et al., 2015).

2.2 | GPS telemetry data

A total of 20 reproductively mature female red deer were selected for the study. The hinds had an average weight of 67.1 (±11.3) kg. These red deer were caught and fitted with Vertex Plus GPS collars from Vectronic Aerospace GmbH in the winter of 2017/2018 using two different approaches. In the first approach, red deer were attracted to an enclosure by food (apple pomace, sugar beets). Within the enclosure, the deer were captured, and GPS collars were attached without chemical immobilization. A second approach was to tranquillise deer using an immobilization gun, with the Hellabrunner mixture (Ketamin and Xylazine) on sites where they were attracted by food. All of the experimental procedures involving animals were approved by the Ethics Committee of the Government of Upper Bavaria (permit number: 55.2Vet-2532.Vet_02–17-190 and 55.2-1-54-2531-82-10).

The GPS collars used were equipped with 6-bit GSM and VHF radio communication capacity as well as GPS sensors (Vectronic Aerospace, Berlin). Collars were programmed to record the positions of red deer with 1 h time intervals between successive fixes. We removed recordings if positional dilution of precision exceeded 10 (D'eon & Delparte, 2005) or velocities between successive locations exceeded 6.5 m/s. For this study, we recorded locations from the beginning of June to the end of September in 2018 and 2019. However, there were six deer whose movement data in the summer of 2019 were missing due to collar malfunction. This resulted in an average of 2554 (±448) locations for six individuals and an average of 5157 (±190) locations for 14 individuals for the analysis.

2.3 | LiDAR data

TLS data were gathered over the summer (July or August) of 2016, 2017 and 2019, respectively, using a RIEGL VZ-400 3D terrestrial scanner (Riegl LMS GmbH, Table 1). In total, we scanned 93 forest plots, representing the main forest types and developmental stages of stands within the park, each with a radius of 20 to 30 m. The central location of each plot was measured using a Leica GPS 1200 with a spatial accuracy of approximately 5–10 cm. To reduce the occlusion effect, we collected four scans for each plot, with one scan in the centre of the plot, and three on the edge of the plot. We placed 12–14 artificial retro-reflective targets in the plot to use as control points for georeferencing and co-registration of multiple scans.

The ALS data were acquired in June 2017 using a Riegl LMSQ 680i instrument, which was carried by helicopter (Table 1). It covers the entire national park with an average point density of 30 points/m^2. The vertical and horizontal accuracy of the ALS data, verified by geometric control using polygons of flat buildings, was 6 and 5 cm, respectively. As a result, the TLS data can be spatially co-registered to ALS data with the vertical and planimetric displacement between the two less than 15 and 16 cm, respectively.

TABLE 1 Specifications for terrestrial LiDAR (TLS) and airborne LiDAR (ALS) data

	Specification	Value
TLS	Sensor	RIEGL VZ-400
	Wavelength	1550 nm
	Beam divergence	0.35 mrad
	Scan angle	Horizontal: 360° Vertical:100° (+60°/−40°)
	Measurement rate	122,000 measurements/second
	Range accuracy	5 mm
	Range	1.5–600 m
ALS	Sensor	Riegl LMSQ 680i
	Wavelength	1550 nm
	Beam divergence	0.5 mrad
	Flying altitude	550 m
	Side lap of parallel flight strips	60%

2.4 | Mapping habitat visibility with LiDAR

As shown by the workflow in Figure 2, we combined TLS and ALS to contiguously measure fine-scale habitat visibility in the study area for red deer using the methods proposed by Zong et al. (2021b, 2021a). First, habitat visibility was estimated from TLS data at the plot level with four major steps. Then, five metrics were calculated from ALS data. Finally, the TLS-based fine-scale visibility was regressed on ALS metrics using the Random Forest algorithm to generate a contiguous visibility map. The code and sample dataset used to generate the fine-scale LiDAR-based visibility were made available in the Dryad repository: DOI https://doi.org/10.5061/dryad.tx95x6b21.

2.4.1 | Estimating visibility from TLS

Visibility at the plot level was estimated by 3D viewshed analysis. Viewshed analysis is normally conducted by testing if the components block the line of sight between an observer and a target in

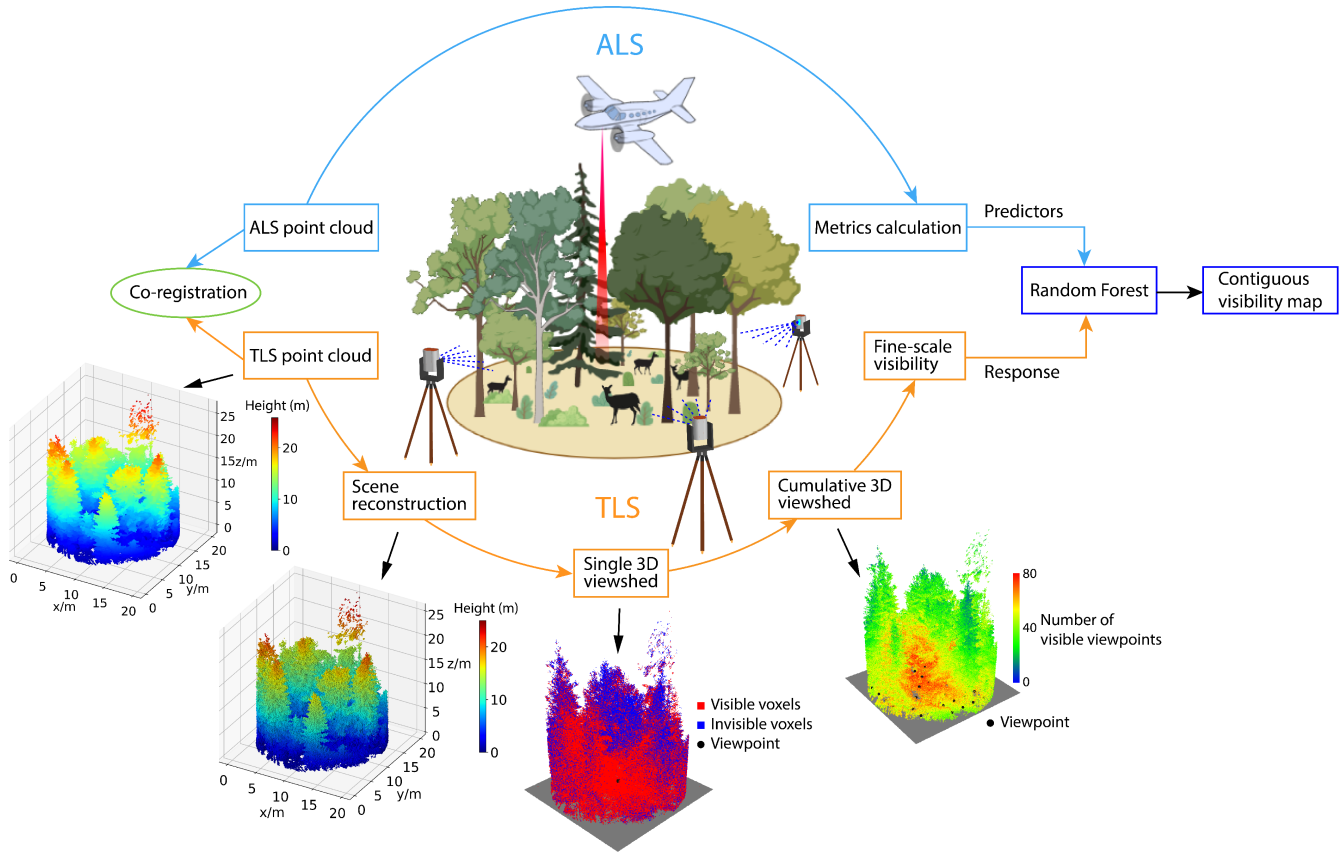

FIGURE 2 Workflow to continuously map fine-scale habitat visibility in forested landscapes by combining terrestrial LiDAR (TLS) and airborne LiDAR (ALS).

the modelled environmental scene (Burrough & McDonnell, 1998). Rather than testing the obstruction of lines of sight typical across surface models in GIS, we operated lines-of-sight analysis in 3D voxel-based models (Figure 2) reconstructed from the TLS point cloud using the occupancy grid algorithm.

First, the space of a TLS plot was divided into a regular grid of 3D voxels, and every voxel was determined to be either 'empty' or 'occupied' by tracing each TLS laser beam through the pre-defined voxel grid. The more laser beams that 'hit' a voxel, the higher the probability of its being occupied, whereas the more laser beams that 'pass through' a voxel, the higher the likelihood of its being empty. We set the side length of the voxel as 10 cm, as recommended by Zong et al. (2021b), and the plot size was 35 × 35 m, which has been proven optimal for temperate forests by Zong et al. (2021a). The habitat visibility from the ground to 2 m high was calculated as this height range enables adult red deer to examine their environment for potential predators while feeding or being vigilant (head up). Therefore, we extracted a subset of point clouds from 0 to 2 m above the ground within the 35 × 35 m square plot for the reconstruction of the scene. In addition, to prevent lines of sight from penetrating the ground in the following lines-of-sight tracing procedure, we generated a digital terrain model (DTM) from TLS points classified as the ground for each plot and combined it with the obtained occupancy grid model.

Second, we created a single 3D viewshed from a specified viewpoint for each plot, by tracing the lines of sight between every voxel in the occupancy grid model and the viewpoint. We assumed that a line of sight will pass through empty voxels until it is obstructed by an occupied voxel, a boundary of the occupancy grid model, or the DTM. After tracing all lines of sight, each voxel in the occupancy grid model will be classified as either 'visible' or 'invisible' depending on whether it is hit by a line of sight. All visible voxels form the single 3D viewshed of a plot from the designated viewpoint (Figure 2).

The single 3D viewshed for a plot is viewpoint specific and thus changes as one moves around the plot. To account for this movement, we repeatedly calculated the 3D viewsheds from 225 viewpoints and summed them into a 3D cumulative viewshed for each plot (Figure 2), which indicates the number of viewpoints from which every voxel is visible, that is, its cumulative visibility. The 225 (25 × 25) viewpoints were distributed in a grid pattern inside the plot, equally spaced northwards and eastwards at a specified eye height of red deer. The number of viewpoints was a trade-off between accuracy and computational cost (Zong et al., 2021a). To account for the difference in the eye height of standing or bedded red deer, we set the height of viewpoints as 140 cm and 30 cm, respectively. Then, the two cumulative viewsheds for different positions of red deer were averaged into a final cumulative viewshed for each plot.

Finally, we normalized the cumulative visibility of each voxel based on the total number of viewpoints, that is, the proportion of visible viewpoints in 225 viewpoints. Then we calculated the average normalized cumulative visibility of all voxels in a plot scene and this defined the fine-scale visibility of the whole plot.

2.4.2 | Up-scaling TLS-based visibility using ALS

As Zong et al. (2021a) have demonstrated, five ALS-derived metrics provided the most accurate predictions of fine-scale visibility at a 35 m resolution in temperate forests using the Random Forest algorithm. These metrics were as follows: 10th height percentiles of canopy returns, 70th height percentiles of understory returns, normalized relative point density (NRD), percentage of NRD and coefficient of variation of 99th height percentiles of understory returns. We extracted the five ALS metrics with a 35 m resolution and put them into the calibrated optimal Random Forest model to continuously map fine-scale visibility over the whole park.

2.5 | Analysis of red deer habitat selection and movement in relation to visibility

2.5.1 | Integrated step selection function

We analysed red deer habitat selection and movement behaviour using an integrated step selection function (iSSF), which compared used steps (two consecutive GPS locations) with a set of available steps, starting from an observed GPS location and ending at a random coordinate (Avgar et al., 2016; Fortin et al., 2005). We paired 10 available steps to each used step (i.e. 11 steps per stratum) using functions within the AMT package in R statistical software (Signer et al., 2019). For our iSSF, we generated available steps using a parameterized gamma distribution of the observed step lengths and the von Mises distribution to the turn angles of the deer in our dataset (Avgar et al., 2016; Forester et al., 2009). After generating random steps, we removed the invalid used-available strata where either the used step or more than four random steps occurred in areas for which covariate data was unavailable (i.e. outside the study area). The resulting dataset comprised 401,569 steps from 20 individuals.

2.5.2 | Model covariates

In addition to fine-scale visibility, we included environmental covariates that are expected to influence habitat selection and movement of red deer as well as three covariates that describe movement attributes of red deer (Table 2).

Topography and land use can influence habitat selection and movement by red deer (Frair et al., 2005; Godvik et al., 2009). We generated the DTM of the study area with a resolution of 10 m based on the classified ground ALS points. To measure terrain ruggedness, we calculated the terrain ruggedness index (Riley et al., 1999) from the ALS-derived DTM. We divided the land use map supplied by

TABLE 2 Variables incorporated in the integrated step selection function of red deer habitat selection and movement

Name	Covariates	Description
Visibility	Fine-scale habitat visibility	3D cumulative visibility derived from LiDAR data
Canopy_cover	Canopy cover	The proportion of all returns with height >2.0 m above-ground within a 35×35 m plot
Land_use	Land use	The land use of the study area was classified into coniferous forest, deciduous forest, mixed forest, deadwood, meadow and bare ground
Elevation	Terrain elevation	DTM generated with a resolution of 10 m from ALS data
Ruggedness	Terrain ruggedness	Terrain ruggedness index calculated from DTM
Time_day	Time of day	Steps were classified as 'day', 'night' and 'twilight'
Step_length	Step length	The distance between two consecutive GPS fixes
ln(Step_length)	Natural logarithm of step length	The natural logarithm of step length
cos(Turn_angle)	Cosine of turn angle	The angle between two consecutive steps

the park into six habitat types: coniferous forest, deciduous forest, mixed forest, deadwood, meadow and bare ground, by merging habitat classes from the original maps (see Silveyra Gonzalez et al., 2018 for a description of the classification of the habitat types). Bare ground class includes roads, railways and residential areas. A study regarding the distribution of forage mass for ungulates in the same park found that herbaceous forage was related to canopy openness (Ewald, Braun, et al., 2014). Therefore, we calculated canopy cover from ALS data with a resolution of 35 m as the proportion of all returns with height >2.0 m above ground.

We included step length, the natural logarithm of step length and turning angle to reduce bias in selection estimates (Duchesne et al., 2015; Forester et al., 2009) and to explicitly model the interaction between step length and habitat visibility (Avgar et al., 2016). The time of day was included as red deer were found to move and choose their habitat differently during different periods of the day (Ensing et al., 2014). A time-of-day category roughly corresponding to daylight, crepuscular light and darkness was calculated to capture the temporal behavioural differences. Steps occurring between 1 h before the sunset and the civil dusk or between the civil dawn and 1 h after sunrise were classified as 'twilight' (crepuscular). Steps classified as 'day' occurred between 1 h after sunrise and 1 h before sunset, and steps taken between the civil dusk and civil dawn were assigned to the 'night' class.

2.6 | Statistical analysis

We constructed generalized linear mixed models (GLMMs) using the glmmTMB package (Brooks et al., 2017) to fit the iSSF containing our variables of interest and interactions between some variables. The full model is listed below:

$$\begin{aligned}\text{Use} \sim\ & \text{Visibility\_end}^2 + \text{Time\_day}: \\ & (\text{Visibility\_end} + \text{Land\_use} + \text{Step\_length} + \ln(\text{Step\_length})) \\ & + \text{Canopy\_cover} + \text{Elevation} + \text{Ruggedness} + \cos(\text{Turn\_angle}) \\ & + \text{Visibility\_start}: (\text{Step\_length} + \ln(\text{Step\_length})).\end{aligned}$$

where ':' denotes interactions between two variables, Visibility_end is the visibility value extracted at the end of a step and Visibility_start is the visibility value extracted at the start of a step. We included a quadratic term for visibility to allow for non-linearity and threshold effects. To evaluate how well a quadratic term fitted the nonlinear relationship (between visibility and red deer locations), we produced used-habitat calibration plots introduced by Fieberg et al. (2018), which provide a way to validate models by comparing the distributions of the explanatory variables at the observed and predicted location. Since we expect that the step length and the selection of visibility and land use of red deer will differ among the periods of the day, we included the interactions between Time_day and these variables. In addition, to test the response regarding the step length of red deer when exposed to certain habitat visibility, we included the interaction of step length and the visibility at the start of a step. We included random intercepts and random slopes for all main effects. We fixed the random intercept variance to 10^6, following the framework proposed by Muff et al. (2020) to avoid shrinkage and subsequent bias. Random slopes avoid bias of model coefficients and standard errors arising from the autocorrelation of GPS observations within each animal and allow the estimation of selection to vary among different individuals. In addition, to avoid multi-collinearity (O'Brien, 2007) in our model, we calculated generalized variance inflation factors between variables using the 'vif' function in the car package of R (Fox & Weisberg, 2018, see Table S1). We then conducted *k*-fold ($k = 5$) cross-validation on our model and calculated Spearman rank correlation (mean of 10 replications) to evaluate model fit based on the methods of Fortin et al. (2009).

Effect sizes of habitat features are reported as relative selection strength (RSS) for one location in the landscape relative to another reference location, given the difference in a variable of interest between the two locations while holding the values of all other variables in the model constant (Avgar et al., 2017). To understand how strongly visibility may influence deer movement rates regardless of habitat selection, the expected step length was calculated by using the iSSF coefficients to adjust the initially observed von Mises and gamma distributions (Avgar et al., 2016; Fieberg et al., 2021).

3 | RESULTS

3.1 | LiDAR-derived fine-scale habitat visibility at the landscape level

Figure 3 illustrates the contiguous map of the fine-scale visibility of the whole study area with a spatial resolution of 35 m, with the visibility of bare ground being the highest (Figure 4). The mean and minimum visibility levels of meadows are both significantly higher compared to the other four forested habitats. The mean visibility of coniferous, deciduous, and mixed forests is at a similar level and is relatively higher than that of deadwood.

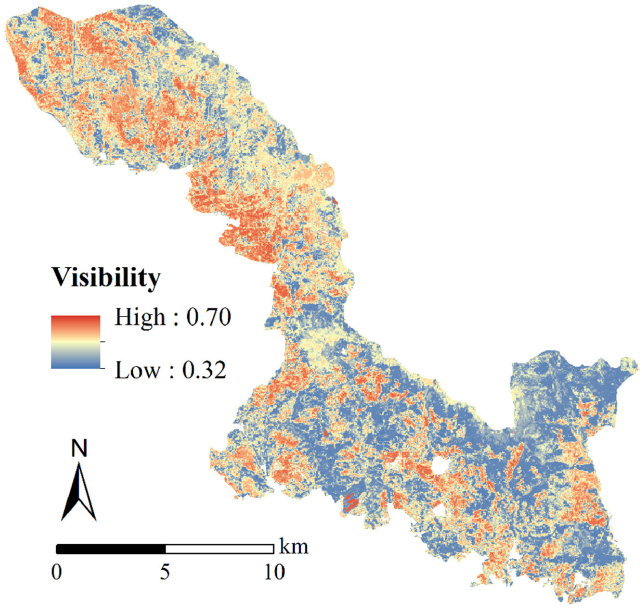

FIGURE 3 Fine-scale visibility map of the Bavarian Forest National Park generated using terrestrial LiDAR (TLS) and airborne LiDAR (ALS) data.

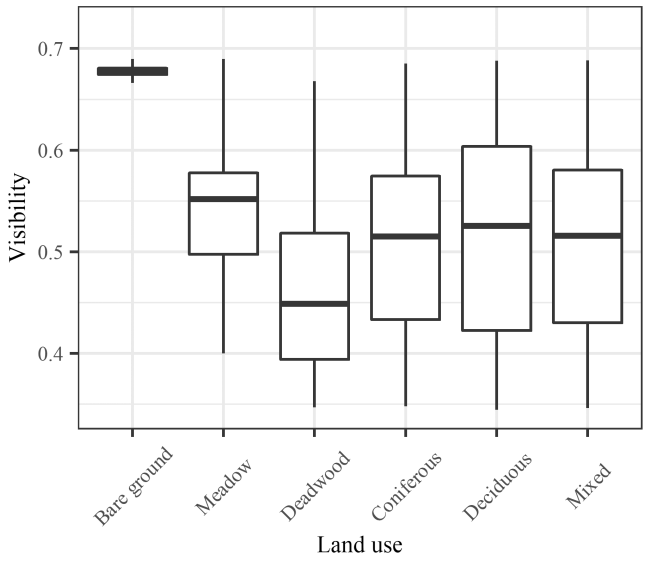

FIGURE 4 Box and whiskers representing fine-scale visibility for various land use.

3.2 | Red deer movement and habitat selection

Parameter coefficients and standard errors for our model are shown in Table 3. *K*-fold cross-validation of our model demonstrated that our model was more significant than random at predicting where red deer moved—the mean Spearman rank correlation coefficient was 0.96 for observed steps.

3.2.1 | Red deer habitat selection in relation to habitat visibility

The RSS rose as habitat visibility approached a certain level but declined with further increases during all three time periods of the day, showing a hump-shaped selection pattern of habitat visibility by red deer (Figure 5). The most preferred visibility level was 0.28 for daytime, whereas the most preferred visibility level was approximately 0.55 for both night and twilight. Selection for visibility was not significantly different between night and twilight as the two standard deviation intervals of RSS always overlap with each other. In addition, the used-habitat calibration plot (Figure S1) indicates that a quadratic term fitted the nonlinear relationship between visibility and the used locations of red deer well.

3.2.2 | Red deer movement in relation to habitat visibility

As the visibility at the start point of a step increased from 0.3 to 0.7, the expected 1-h step length of red deer increased more or less exponentially from 53 to 121 m, from 66 to 158 m, and from 116 to 374 m, during the day, night and twilight, respectively (Figure 6). In addition, the expected 1-h step length of deer was significantly higher during twilight than that during daytime and night. There was no significant difference in the expected 1-h step length between night and twilight.

4 | DISCUSSION

In this paper, we employed a newly described method that combines terrestrial and airborne LiDAR to continuously measure the fine-scale habitat visibility at the landscape level in forest ecosystems. We then applied the LiDAR-derived visibility to investigate how a forest dweller (i.e. red deer) selects visibility and adjusts its movement accordingly on a home-range scale. We found that red deer selected intermediate habitat visibility throughout the day and night. Their preferred level of visibility during daylight was lower than that during night and twilight, whereas the preference was not

TABLE 3 Coefficient estimates, standard errors (SE), and *p* values for the integrated step selection function of red deer habitat selection and movement.

Covariates	Coefficient	SE	*p* value	Significance
Visibility_end^2	−11.41	2.82	0.000	***
Visibility_end:Day	6.39	2.57	0.031	*
Visibility_end:Night	12.59	3.02	0.000	***
Visibility_end:Twilight	12.55	3.03	0.000	***
Bare Ground:Day	−1.79	0.76	0.019	*
Bare Ground:Night	−0.54	0.26	0.039	*
Bare Ground:Twilight	−0.32	0.43	0.454	
Coniferous:Day	0.18	0.24	0.447	
Coniferous:Night	−0.83	0.16	0.000	***
Coniferous:Twilight	−0.56	0.27	0.037	*
Deadwood:Day	0.41	0.22	0.048	*
Deadwood:Night	−0.26	0.12	0.030	*
Deadwood:Twilight	−0.21	0.18	0.245	
Deciduous:Day	0.52	0.21	0.014	*
Deciduous:Night	−0.70	0.15	0.000	***
Deciduous:Twilight	−0.59	0.20	0.003	**
Mixed:Day	0.34	0.24	0.168	
Mixed:Night	−0.85	0.11	0.000	***
Mixed:Twilight	−0.58	0.23	0.014	*
Canopy_cover	−0.86	0.11	0.000	***
Elevation	−0.00046	0.0005	0.363	
Ruggedness	−0.05	0.008	0.000	***
Step_length:Day	−0.0067	0.00073	0.000	***
Step_length:Night	−0.0059	0.00069	0.000	***
Step_length:Twilight	−0.0036	0.00060	0.000	***
ln(Step_length):Day	−0.15	0.038	0.000	***
ln(Step_length):Night	−0.076	0.049	0.126	
ln(Step_length):Twilight	0.11	0.052	0.034	*
Step_length:Visibility_start	0.01	0.0011	0.000	***
ln(Step_length):Visibility_start	0.40	0.082	0.000	***
cos(Turn_angle)	−0.0091	0.012	0.441	

*, ** and *** indicate statistical significance at $p<0.05$, $p<0.01$ and $p<0.001$, respectively

significantly different between night and twilight. In addition, red deer moved faster in areas with high visibility at all times of the day. Furthermore, red deer most rapidly transited between locations in the twilight.

The hump-shaped selection pattern of habitat visibility by red deer might arise from multiple factors. First, the trade-off between food availability and predation risk (Gower et al., 2008; Lone et al., 2015; Ripple & Beschta, 2003) limits the time spent by red deer in both open and closed habitats. In addition, to reduce being exposed to more intense human disturbance during daylight compared to darkness, red deer have been observed to use more open forage-rich habitats during darkness, and covered habitats with less forage during daylight (Godvik et al., 2009; Green & Bear, 1990). The red deer population in our study area has shown the same habitat selection pattern where meadows were preferred compared to various types of forested habitats (i.e. coniferous, deciduous, and mixed forest and deadwood) during both twilight and night, whereas forests were more used than meadows during daylight (Table 3 and Figure S2a). Consequently, the most preferred level of visibility by deer during daylight was substantially lower than that during night and twilight, as the visibility of meadows is higher than in forested habitats (Figure 4). It is worth noting that the 1-h GPS fix frequency in our study is relatively coarse compared to the 4-h duration of the twilight periods (i.e. 2 h during dawn and dusk, respectively). Thus, some behaviour of the red deer at finer temporal scales could have been hidden. This might be used to partially explain why we found no significant difference in the selection for habitat visibility by red deer between night and twilight in our analysis. Nonetheless, the spatial resolution of our visibility map is high, which can be used to support analyses with much finer temporal resolution GPS tracking

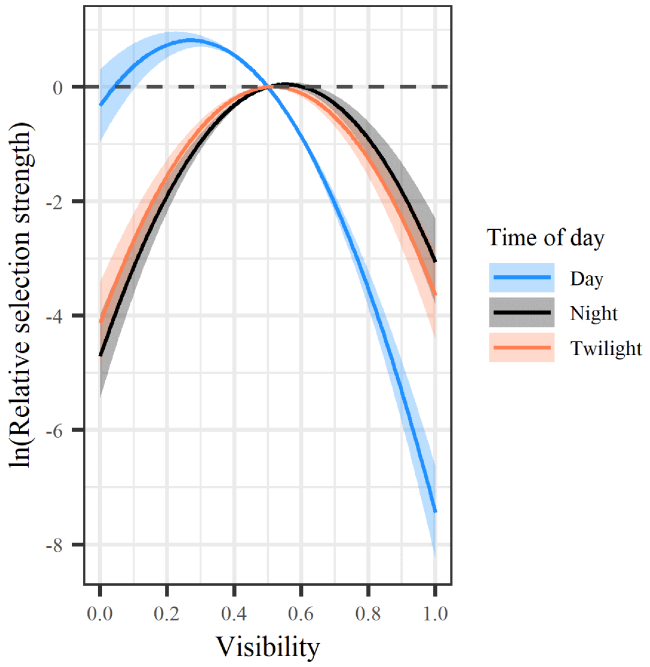

FIGURE 5 The natural logarithm of relative selection strength (Avgar et al., 2017) of fine-scale visibility by red deer during the day (blue), night (black) and twilight (red), with the reference visibility value as 0.5. The plotted lines represent the relative probability of selection, and the shaded areas are standard errors. The dotted horizontal line denotes no response, whereas values above that line indicate selection for and values below that line indicate avoidance against habitat.

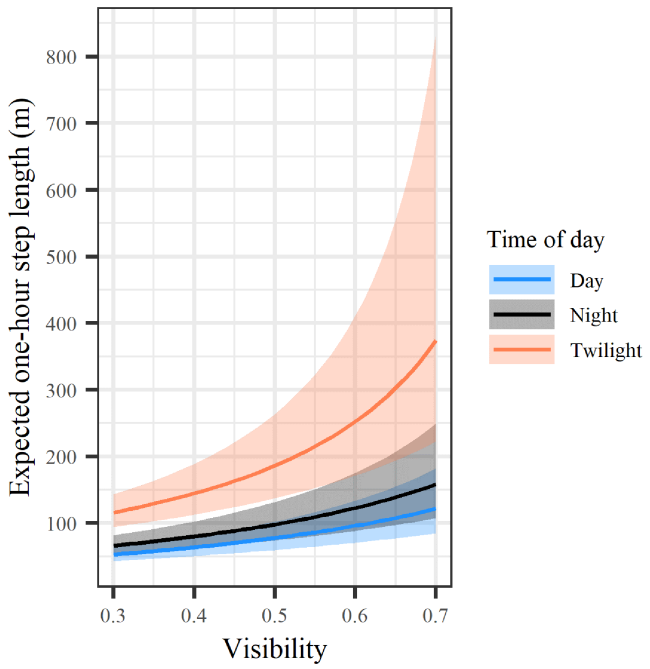

FIGURE 6 Expected movement rate changes with fine-scale habitat visibility at the start point of a step by red deer during the day (blue), night (black) and twilight (red). The plotted lines represent the expected 1-h step length, and the shaded areas are standard errors.

data. Second, the interaction between habitat visibility and hunting modes of predators is presumably another driving factor. A high degree of visibility might increase the detection of predators; however, it also implies low concealment cover, which tends to increase prey detectability (Camp et al., 2013; Olsoy et al., 2014). In open habitats, predation risk from humans counting on long lines of sight is high (Farmer et al., 2006; Norum et al., 2015), whereas, in covered habitats with low visibility, it is more difficult for red deer to detect an approaching lynx, a stalking predator in the study area (Ewald, Dupke, et al., 2014; Filla et al., 2017). Therefore, to prevent predation from hunters and lynx in areas of higher risk, red deer avoid extremely high and low habitat visibility. Furthermore, very low visibility often implies the presence of more objects on the ground, which potentially impose more escape impediments to red deer, and thus the habitats with low visibility were avoided. For example, it has been proven that tree logs or rocks can reduce visibility and hinder escape movement for ungulates (Halofsky & Ripple, 2008; Kuijper et al., 2015). Finally, as shown in Figure 4, the areas with intense human activities such as roads and residential areas usually have high visibility (i.e. low concealment).

The avoidance of areas with extremely low and high visibility as shown in the used-habitat calibration (Figure S1) suggests that a quadratic effect of visibility might be needed. Given the quadratic term for visibility included in the iSSF model, the distribution of visibility values at the observed locations largely fell within the 95% simulation envelope, indicating that this model was well-calibrated. Nonetheless, it is noteworthy that compared to nonparametric types of regression such as generalized additive models and classification trees, GLMM approach is bound to clear but rather limited parametric shapes. Therefore, although a quadratic term was enough to fit the nonlinear relationship between visibility and space use of red deer in our study well, using polynomials of higher orders or even fitting a more flexible model with a nonparametric approach is possible if the species of interest behave in a more complex manner in response to habitat visibility.

The preference for intermediate fine-scale visibility implies that red deer make a trade-off between visibility and concealment, which are the opposing functional properties of the habitat and influence predation risk. Although visibility inversely relates to concealment, the correlation is not necessarily one to one, which allows the prey to balance between the two to gain more of one while giving up relatively less of the other (Camp et al., 2013; Olsoy et al., 2014). Similar to red deer, pygmy rabbits *Brachylagus idahoensis* have been observed to make a trade-off between visibility and concealment in a shrub-steppe habitat at small scales (Camp et al., 2013). It has been well documented that foraging animals seek concealment cover when exposed to high predation risk (Chassagneux et al., 2020; Mysterud & Østbye, 1999; Stankowich & Blumstein, 2005), but open lines of sight can also reduce perceptions of predation risk by herbivores (Altendorf et al., 2001; Embar et al., 2011; Ripple & Beschta, 2003). Most likely, the trade-off between visibility and concealment might be practiced by other forest-dwelling foragers when making decisions on location choice (Aben et al., 2018; Lima

& Dill, 1990), with the balance between the two likely to be species specific and even context dependent for specific species. The relative importance of concealment versus open lines of sight can depend on the characteristics of the animal, its activities, potential predators, habitat types and environmental factors, such as weather and light conditions (Arenz & Leger, 1997; Lima & Dill, 1990). For example, it might be expected that a forager with weak locomotion ability may trade more visibility for concealment as it cannot flee to refuge fast even though high visibility allows it to detect approaching predators early. Due to the absence of methods to efficiently quantify fine-scale habitat visibility in a heterogeneous landscape, especially in a continuous way, the investigation of the trade-off between visibility and concealment for herbivore animals remains extremely limited. To our knowledge, this is the first time that the preference for intermediate fine-scale visibility by a forest-dwelling herbivore at a landscape scale was revealed, which is feasible thanks to the LiDAR technique. As stated in the study of Camp et al. (2013), because visibility for pygmy rabbits was measured using obscurity boards over a limited spatial extent relative to the high heterogeneity of the habitat, the significance of the revealed relationship between visibility and concealment was undermined. Here, we highlight the opportunity to use the continuous map of fine-scale visibility derived from LiDAR in conjunction with animal tracking data to refine our understanding of the functional relationships between predation risk and habitat visibility and concealment and provide insight into how habitat structure mechanistically relates to predation risk in highly heterogeneous landscapes.

Red deer moved faster in areas with high visibility at all times of the day. We interpret the adaption of red deer movement rate to habitat visibility partially to reduce human disturbance. Red deer have been observed to be more likely to relocate in open areas with higher human and predator risks (Frair et al., 2005; Lone et al., 2015) as well as more intensive human recreational activities (Coppes et al., 2017) to reduce the time spent in such places. In addition, red deer spend more time resting in forested habitats and more often feed, mostly with accompanying forward motion, in open meadow habitats. Another reason might be that highly dense vegetation or rough terrain in areas with low visibility can slow the movement of deer. Furthermore, red deer transited most rapidly between locations in the twilight. This is consistent with the fact that red deer spend more time foraging and moving between resting and feeding sites during twilight hours (Green & Bear, 1990).

The preference for low canopy cover by red deer (Table 3 and Figure S2b) is probably associated with higher food availability in areas with lower canopy cover. Ewald, Braun, et al. (2014) found a moderately negative relationship between herbaceous forage for ungulates and canopy cover in Bavarian Forest National Park. In addition, the preference for low canopy cover by red deer observed in our study is in line with the previous findings that habitat suitability for red deer consistently improved after forest disturbances including bark beetle infestations, windthrows and logging (Oeser et al., 2021), which usually cause a substantial decrease in canopy cover. The strong selection of rugged terrain by lynx in our study area (Filla et al., 2017) may be one reason why red deer avoided high terrain ruggedness (Table 3 and Figure S2c). Another possible reason is that the movement of deer is hindered and therefore deer are more prone to follow paths in rough terrain, so their escape routines are more easily predicted by hunters or predictors (Lone et al., 2014). Elevation has been proven to play an important role in seasonal migration causing a concentration of deer in the valleys in winter mainly because of higher food availability (Mysterud et al., 2017; Rivrud et al., 2016). However, our results suggest that elevation had no significant effects on the summer habitat selection of red deer in our study area. Due to forage abundance for red deer, classified as an intermediate feeder, does not vary significantly along an elevation gradient in summer (Ewald, Braun, et al., 2014), the effect of elevation partially brought by food availability on summer habitat selection of red deer was weakened.

The LiDAR-based approach could provide comparable measurements of visibility (i.e. 3D cumulative viewshed) among studies. It is difficult to compare visibility measurements obtained by obscurity board-based methods and various surrogate metrics across studies conducted in various terrestrial ecosystems (Moll et al., 2017). For obscurity board-based methods, various factors, such as board size, distance from the board to the observer and observation direction, might lead to little cross-study comparability. Furthermore, it is impractical to compare different surrogate metrics (e.g. land cover type, topography, vegetation cover and vegetation density) and even to compare the same metric among different ecosystems. For example, although vegetation cover is low in rock outcrop areas with 'rough' local terrain, visibility could be low due to obstruction from rocks. By contrast, the LiDAR-based method calculated 3D viewsheds; therefore, the obstruction effects of all objects on the ground scanned by LiDAR can be accounted for.

In addition, the continuous map of fine-scale visibility over a landscape extent fills in the gaps of resolution where researchers can examine how visibility may shape the spatial variation in predation risk and therefore influence animal habitat selection and movement in terrestrial ecosystems. Furthermore, the visibility measured with 3D cumulative viewshed is widely adaptable for various applications in animal ecological research. First, 3D cumulative viewshed can be calculated from the perspective of not only prey species but also predators and, therefore, holds potential for studying predation behaviour and strategy. In addition, 3D cumulative viewshed can be estimated with different viewing heights to represent different head positions for various animal activities. As in our study, the eye position of red deer when active is higher than when lying down. Thus, 3D cumulative viewshed allows the study of the influence of visibility on behaviour-specific habitat selection of animals. Moreover, scanning angles of animals can be limited within different ranges to measure visibility along only horizontal or vertical directions so that predation risk from terrestrial or avian predators can be quantified, respectively. Therefore, 3D cumulative viewshed can also serve as an efficient tool to investigate the interactions between predators with different hunting domains and the vegetation structure on perceived predation risk by prey species. Here, we advocate adopting

3D cumulative viewshed as a measurement of visibility for animal ecological research.

AUTHOR CONTRIBUTIONS

Conceived and designed the study: Xin Zong, Tiejun Wang and Andrew K. Skidmore. Collected data: Xin Zong and Marco Heurich. Wrote the manuscript: Xin Zong. Reviewed the paper: Tiejun Wang, Andrew Skidmore and Marco Heurich. All authors contributed critically to the drafts and approved the final manuscript.

ACKNOWLEDGEMENTS

The work of the first author was sponsored by the China Scholarship Council (grant number 201704910852). The authors are thankful for the support of the European Research Council (European Commission BIOSPACE—Monitoring Biodiversity from Space project; grant agreement 834709, H2020-EU.1.1.) and the 'Data Pool Initiative' of the Bohemian Forest Ecosystem.

CONFLICT OF INTEREST

None of the authors have a conflict of interest to report.

DATA AVAILABILITY STATEMENT

Data available from the Dryad Digital Repository: https://doi.org/10.5061/dryad.15dv41p1d (Zong et al., 2022).

ORCID

Xin Zong https://orcid.org/0000-0002-1804-1906
Tiejun Wang http://orcid.org/0000-0002-1138-8464
Andrew K. Skidmore http://orcid.org/0000-0002-7446-8429
Marco Heurich http://orcid.org/0000-0003-0051-2930

REFERENCES

Aben, J., Pellikka, P., Travis, J. M. J., & Parrini, F. (2018). A call for viewshed ecology: Advancing our understanding of the ecology of information through viewshed analysis. *Methods in Ecology and Evolution*, *9*, 624–633.

Acebes, P., Malo, J. E., & Traba, J. (2013). Trade-offs between food availability and predation risk in desert environments: The case of polygynous monomorphic guanaco (*Lama guanicoe*). *Journal of Arid Environments*, *97*, 136–142.

Adrados, C., Baltzinger, C., Janeau, G., & Pépin, D. (2008). Red deer Cervus elaphus resting place characteristics obtained from differential GPS data in a forest habitat. *European Journal of Wildlife Research*, *54*(3), 487–494. https://doi.org/10.1007/s10344-008-0174-y

Alonso, J. C., Álvarez-Martínez, J. M., & Palacín, C. (2012). Leks in ground-displaying birds: Hotspots or safe places? *Behavioral Ecology*, *23*, 491–501.

Altendorf, K. B., Laundré, J. W., López González, C. A., & Brown, J. S. (2001). Assessing effects of predation risk on foraging behavior of mule deer. *Journal of Mammalogy*, *82*, 430–439.

Andersson, M., Wallander, J., & Isaksson, D. (2009). Predator perches: A visual search perspective. *Functional Ecology*, *23*, 373–379.

Arenz, C. L., & Leger, D. W. (1997). Artificial visual obstruction, anti-predator vigilance, and predator detection in the thirteen-lined ground squirrel (*Spermophilus tridecemlineatus*). *Behaviour*, *134*, 1101–1114.

Avgar, T., Lele, S. R., Keim, J. L., & Boyce, M. S. (2017). Relative selection strength: Quantifying effect size in habitat-and step-selection inference. *Ecology and Evolution*, *7*, 5322–5330.

Avgar, T., Potts, J. R., Lewis, M. A., & Boyce, M. S. (2016). Integrated step selection analysis: Bridging the gap between resource selection and animal movement. *Methods in Ecology and Evolution*, *7*, 619–630.

Belotti, E., Weder, N., Bufka, L., Kaldhusdal, A., Küchenhoff, H., Seibold, H., Woelfing, B., & Heurich, M. (2015). Patterns of lynx predation at the interface between protected areas and multi-use landscapes in Central Europe. *PLoS One*, *10*, e0138139.

Brooks, M. E., Kristensen, K., Van Benthem, K. J., Magnusson, A., Berg, C. W., Nielsen, A., Skaug, H. J., Machler, M., & Bolker, B. M. (2017). glmmTMB balances speed and flexibility among packages for zero-inflated generalized linear mixed modeling. *The R Journal*, *9*, 378–400.

Burrough, P. A., & McDonnell, R. A. (1998). *Principles of geographical information systems* (p. 346). Oxford University Press.

Cailleret, M., Heurich, M., & Bugmann, H. (2014). Reduction in browsing intensity may not compensate climate change effects on tree species composition in the Bavarian Forest National Park. *Forest Ecology and Management*, *328*, 179–192.

Camp, M., Rachlow, J., Woods, B., Johnson, T., & Shipley, L. (2013). Examining functional components of cover: The relationship between concealment and visibility in shrub-steppe habitat. *Ecosphere*, *4*, 1–14.

Camp, M. J., Rachlow, J. L., Woods, B. A., Johnson, T. R., & Shipley, L. A. (2012). When to run and when to hide: The influence of concealment, visibility, and proximity to refugia on perceptions of risk. *Ethology*, *118*, 1010–1017.

Chassagneux, A., Calenge, C., Marchand, P., Richard, E., Guillaumat, E., Baubet, E., & Saïd, S. (2020). Should I stay or should I go? Determinants of immediate and delayed movement responses of female red deer (*Cervus elaphus*) to drive hunts. *PLoS ONE*, *15*, e0228865.

Ciuti, S., Tripke, H., Antkowiak, P., Gonzalez, R. S., Dormann, C. F., & Heurich, M. (2018). An efficient method to exploit Li DAR data in animal ecology. *Methods in Ecology and Evolution*, *9*, 893–904.

Coppes, J., Burghardt, F., Hagen, R., Suchant, R., & Braunisch, V. (2017). Human recreation affects spatio-temporal habitat use patterns in red deer (*Cervus elaphus*). *PLoS ONE*, *12*, e0175134.

Davies, A. B., Cromsigt, J. P., Tambling, C. J., le Roux, E., Vaughn, N., Druce, D. J., Marneweck, D. G., & Asner, G. P. (2021). Environmental controls on African herbivore responses to landscapes of fear. *Oikos*, *130*, 171–186.

Davies, A. B., Marneweck, D. G., Druce, D. J., & Asner, G. P. (2016). Den site selection, pack composition, and reproductive success in endangered African wild dogs. *Behavioral Ecology*, *27*, 1869–1879.

Davies, A. B., Tambling, C. J., Kerley, G. I., & Asner, G. P. (2016). Effects of vegetation structure on the location of lion kill sites in African thicket. *PLoS ONE*, *11*, e0149098.

D'eon, R. G., & Delparte, D. (2005). Effects of radio-collar position and orientation on GPS radio-collar performance, and the implications of PDOP in data screening. *Journal of Applied Ecology*, *42*, 383–388.

Duchesne, T., Fortin, D., & Rivest, L.-P. (2015). Equivalence between step selection functions and biased correlated random walks for statistical inference on animal movement. *PLoS ONE*, *10*, e0122947.

Dupke, C., Bonenfant, C., Reineking, B., Hable, R., Zeppenfeld, T., Ewald, M., & Heurich, M. (2017). Habitat selection by a large herbivore at multiple spatial and temporal scales is primarily governed by food resources. *Ecography*, *40*, 1014–1027.

Embar, K., Kotler, B. P., & Mukherjee, S. (2011). Risk management in optimal foragers: The effect of sightlines and predator type on patch use, time allocation, and vigilance in gerbils. *Oikos*, *120*, 1657–1666.

Ensing, E. P., Ciuti, S., de Wijs, F. A., Lentferink, D. H., Ten Hoedt, A., Boyce, M. S., & Hut, R. A. (2014). GPS based daily activity patterns in European red deer and north American elk (*Cervus elaphus*): Indication for a weak circadian clock in ungulates. *PLoS ONE*, *9*, e106997.

Ewald, J., Braun, L., Zeppenfeld, T., Jehl, H., & Heurich, M. (2014). Estimating the distribution of forage mass for ungulates from vegetation plots in Bavarian Forest National Park. *Tuexenia*, *34*, 53–70.

Ewald, M., Dupke, C., Heurich, M., Müller, J., & Reineking, B. (2014). LiDAR remote sensing of Forest structure and GPS telemetry data provide insights on winter habitat selection of European roe deer. *Forests*, *5*, 1374–1390.

Fahse, L., & Heurich, M. (2011). Simulation and analysis of outbreaks of bark beetle infestations and their management at the stand level. *Ecological Modelling*, *222*, 1833–1846.

Farmer, C. J., Person, D. K., & Bowyer, R. T. (2006). Risk factors and mortality of black-tailed deer in a managed forest landscape. *The Journal of Wildlife Management*, *70*, 1403–1415.

Fieberg, J. R., Forester, J. D., Street, G. M., Johnson, D. H., ArchMiller, A. A., & Matthiopoulos, J. (2018). Used-habitat calibration plots: A new procedure for validating species distribution, resource selection, and step-selection models. *Ecography*, *41*, 737–752.

Fieberg, J. R., Signer, J., Smith, B., & Avgar, T. (2021). A 'how to' guide for interpreting parameters in habitat-selection analyses. *Journal of Animal Ecology*, *90*, 1027–1043.

Filla, M., Premier, J., Magg, N., Dupke, C., Khorozyan, I., Waltert, M., Bufka, L., & Heurich, M. (2017). Habitat selection by Eurasian lynx (*Lynx lynx*) is primarily driven by avoidance of human activity during day and prey availability during night. *Ecology and Evolution*, *7*, 6367–6381.

Forester, J. D., Im, H. K., & Rathouz, P. J. (2009). Accounting for animal movement in estimation of resource selection functions: Sampling and data analysis. *Ecology*, *90*, 3554–3565.

Fortin, D., Beyer, H. L., Boyce, M. S., Smith, D. W., Duchesne, T., & Mao, J. S. (2005). Wolves influence elk movements: Behavior shapes a trophic cascade in Yellowstone National Park. *Ecology*, *86*, 1320–1330.

Fortin, D., Fortin, M.-E., Beyer, H. L., Duchesne, T., Courant, S., & Dancose, K. (2009). Group-size-mediated habitat selection and group fusion–fission dynamics of bison under predation risk. *Ecology*, *90*, 2480–2490.

Fox, J., & Weisberg, S. (2018). *An R companion to applied regression* (3rd ed.). Sage publications.

Frair, J. L., Merrill, E. H., Visscher, D. R., Fortin, D., Beyer, H. L., & Morales, J. M. (2005). Scales of movement by elk (Cervus elaphus) in response to heterogeneity in forage resources and predation risk. *Landscape Ecology*, *20*, 273–287.

Godvik, I. M. R., Loe, L. E., Vik, J. O., Veiberg, V., Langvatn, R., & Mysterud, A. (2009). Temporal scales, trade-offs, and functional responses in red deer habitat selection. *Ecology*, *90*, 699–710.

Gower, C. N., Garrott, R. A., & White, P. (2008). Elk foraging behavior: Does predation risk reduce time for food acquisition? *Terrestrial Ecology*, *3*, 423–450.

Green, R. A., & Bear, G. D. (1990). Seasonal cycles and daily activity patterns of Rocky Mountain elk. *The Journal of Wildlife Management*, *54*, 272–279.

Halofsky, J. S., & Ripple, W. J. (2008). Fine-scale predation risk on elk after wolf reintroduction in Yellowstone National Park, USA. *Oecologia*, *155*, 869–877.

Higgins, K. F., Oldemeyer, J., Jenkins, K., Clambey, G., & Harlow, R. (1996). Vegetation sampling and Measurement. *Research and Management Techniques for Wildlife and Habitats*, *5*, 567–591.

Hopcraft, J. G. C., Sinclair, A. R. E., & Packer, C. (2005). Planning for success: Serengeti lions seek prey accessibility rather than abundance. *Journal of Animal Ecology*, *74*, 559–566.

Jarnemo, A., & Wikenros, C. (2014). Movement pattern of red deer during drive hunts in Sweden. *European Journal of Wildlife Research*, *60*, 77–84.

Johnson, B. K., Kern, J. W., Wisdom, M. J., Findholt, S. L., & Kie, J. G. (2000). Resource selection and spatial separation of mule deer and elk during spring. *The Journal of Wildlife Management*, *64*, 685–697.

Johnson, D. H. (1980). The comparison of usage and availability measurements for evaluating resource preference. *Ecology*, *61*, 65–71.

Kuijper, D. P., Bubnicki, J. W., Churski, M., Mols, B., & Van Hooft, P. (2015). Context dependence of risk effects: Wolves and tree logs create patches of fear in an old-growth forest. *Behavioral Ecology*, *26*, 1558–1568.

Lecigne, B., Eitel, J. U., & Rachlow, J. L. (2020). viewshed3d: An r package for quantifying 3D visibility using terrestrial lidar data. *Methods in Ecology and Evolution*, *11*, 733–738.

Lima, S. L., & Dill, L. M. (1990). Behavioral decisions made under the risk of predation: A review and prospectus. *Canadian Journal of Zoology*, *68*, 619–640.

Loarie, S. R., Tambling, C. J., & Asner, G. P. (2013). Lion hunting behaviour and vegetation structure in an African savanna. *Animal Behaviour*, *85*, 899–906.

Lone, K., Loe, L. E., Gobakken, T., Linnell, J. D., Odden, J., Remmen, J., & Mysterud, A. (2014). Living and dying in a multi-predator landscape of fear: Roe deer are squeezed by contrasting pattern of predation risk imposed by lynx and humans. *Oikos*, *123*, 641–651.

Lone, K., Loe, L. E., Meisingset, E. L., Stamnes, I., & Mysterud, A. (2015). An adaptive behavioural response to hunting: Surviving male red deer shift habitat at the onset of the hunting season. *Animal Behaviour*, *102*, 127–138.

Moll, R. J., Redilla, K. M., Mudumba, T., Muneza, A. B., Gray, S. M., Abade, L., Hayward, M. W., Millspaugh, J. J., & Montgomery, R. A. (2017). The many faces of fear: A synthesis of the methodological variation in characterizing predation risk. *Journal of Animal Ecology*, *86*, 749–765.

Möst, L., Hothorn, T., Müller, J., & Heurich, M. (2015). Creating a landscape of management: Unintended effects on the variation of browsing pressure in a national park. *Forest Ecology and Management*, *338*, 46–56.

Muff, S., Signer, J., & Fieberg, J. (2020). Accounting for individual-specific variation in habitat-selection studies: Efficient estimation of mixed-effects models using Bayesian or frequentist computation. *Journal of Animal Ecology*, *89*, 80–92.

Mysterud, A., & Østbye, E. (1999). Cover as a habitat element for temperate ungulates: Effects on habitat selection and demography. *Wildlife Society Bulletin*, *27*, 385–394.

Mysterud, A., Vike, B. K., Meisingset, E. L., & Rivrud, I. M. (2017). The role of landscape characteristics for forage maturation and nutritional benefits of migration in red deer. *Ecology and Evolution*, *7*, 4448–4455.

Norum, J. K., Lone, K., Linnell, J. D., Odden, J., Loe, L. E., & Mysterud, A. (2015). Landscape of risk to roe deer imposed by lynx and different human hunting tactics. *European Journal of Wildlife Research*, *61*, 831–840.

O'brien, R. M. (2007). A caution regarding rules of thumb for variance inflation factors. *Quality & Quantity*, *41*, 673–690.

Oeser, J., Heurich, M., Senf, C., Pflugmacher, D., & Kuemmerle, T. (2021). Satellite-based habitat monitoring reveals long-term dynamics of deer habitat in response to forest disturbances. *Ecological Applications*, *31*, e2269.

Olsoy, P. J., Forbey, J. S., Rachlow, J. L., Nobler, J. D., Glenn, N. F., & Shipley, L. A. (2014). Fearscapes: Mapping functional properties of cover for prey with terrestrial LiDAR. *Bioscience*, *65*, 74–80.

Proffitt, K. M., Grigg, J. L., Hamlin, K. L., & Garrott, R. A. (2009). Contrasting effects of wolves and human hunters on elk behavioral responses to predation risk. *The Journal of Wildlife Management*, *73*, 345–356.

Rearden, S. N., Anthony, R. G., & Johnson, B. K. (2011). Birth-site selection and predation risk of Rocky Mountain elk. *Journal of Mammalogy*, *92*, 1118–1126.

Riley, S. J., DeGloria, S. D., & Elliot, R. (1999). Index that quantifies topographic heterogeneity. *Intermountain Journal of Sciences*, *5*, 23–27.

Ripple, W. J., & Beschta, R. L. (2003). Wolf reintroduction, predation risk, and cottonwood recovery in Yellowstone National Park. *Forest Ecology and Management*, *184*, 299–313.

Rivrud, I. M., Heurich, M., Krupczynski, P., Müller, J., & Mysterud, A. (2016). Green wave tracking by large herbivores: An experimental approach. *Ecology*, *97*, 3547–3553.

Röder, J., Bässler, C., Brandl, R., Dvořak, L., Floren, A., Goßner, M. M., Gruppe, A., Jarzabek-Müller, A., Vojtech, O., & Wagner, C. (2010). Arthropod species richness in the Norway Spruce (*Picea abies* (L.) karst.) canopy along an elevation gradient. *Forest Ecology and Management*, *259*, 1513–1521.

Salvatori, M., De Groeve, J., van Loon, E., De Baets, B., Morellet, N., Focardi, S., Bonnot, N., Gehr, B., Griggio, M., & Heurich, M. (2022). Day versus night use of forest by red and roe deer as determined by Corine Land Cover and Copernicus Tree Cover Density: Assessing use of geographic layers in movement ecology. *Landscape Ecology*, *37*, 1453–1468.

Signer, J., Fieberg, J., & Avgar, T. (2019). Animal movement tools (amt): R package for managing tracking data and conducting habitat selection analyses. *Ecology and Evolution*, *9*, 880–890.

Silveyra Gonzalez, R., Latifi, H., Weinacker, H., Dees, M., Koch, B., & Heurich, M. (2018). Integrating LiDAR and high-resolution imagery for object-based mapping of forest habitats in a heterogeneous temperate forest landscape. *International Journal of Remote Sensing*, *39*, 8859–8884.

Stankowich, T., & Blumstein, D. T. (2005). Fear in animals: A meta-analysis and review of risk assessment. *Proceedings of the Royal Society B: Biological Sciences*, *272*, 2627–2634.

Tandy, C. R. V. (1967). The isovist method of landscape survey. In H. C. Murray (Ed.), *Methods of landscape analysis* (pp. 9–10). UK: Landscape Research Group.

Wiens, J. A. (1989). Spatial scaling in ecology. *Functional Ecology*, *3*, 385–397.

Zong, X., Wang, T., Skidmore, A. K., & Heurich, M. (2021a). Estimating fine-scale visibility in a temperate forest landscape using airborne laser scanning. *International Journal of Applied Earth Observation and Geoinformation*, *103*, 102478.

Zong, X., Wang, T., Skidmore, A. K., & Heurich, M. (2021b). The impact of voxel size, forest type, and understory cover on visibility estimation in forests using terrestrial laser scanning. *GIScience & Remote Sensing*, *58*(3), 1–17.

Zong, X., Wang, T., Skidmore, A., & Heurich, M. (2022). Data from: LiDAR reveals a preference for intermediate visibility by a forest-dwelling ungulate species. *Dryad Digital Repository*. https://doi.org/10.5061/dryad.15dv41p1d

SUPPORTING INFORMATION

Additional supporting information can be found online in the Supporting Information section at the end of this article.

How to cite this article: Zong, X., Wang, T., Skidmore, A. K., & Heurich, M. (2022). LiDAR reveals a preference for intermediate visibility by a forest-dwelling ungulate species. *Journal of Animal Ecology*, *00*, 1–14. https://doi.org/10.1111/1365-2656.13847